



Three-Dimensional Modeling of Thyroid Hormone Metabolites Binding to the Cancer-Relevant $\alpha\beta 3$ Integrin: *In-Silico* Based Study

Dror Tobi^{1,2*}, Eilon Krashin^{3,4†}, Paul J. Davis^{5,6}, Vivian Cody⁷, Martin Ellis^{3,8,9} and Osnat Ashur-Fabian^{3,4,8*}

¹ Department of Molecular Biology, Ariel University, Ariel, Israel, ² Department of Computer Sciences, Ariel University, Ariel, Israel, ³ Translational Oncology Laboratory, Meir Medical Center, Kfar-Saba, Israel, ⁴ Department of Human Molecular Genetics and Biochemistry, Sackler School of Medicine, Tel Aviv University, Tel Aviv, Israel, ⁵ Department of Medicine, Albany Medical College, Albany, NY, United States, ⁶ Pharmaceutical Research Institute, Albany College of Pharmacy and Health Sciences, Albany, NY, United States, ⁷ Hauptman-Woodward Medical Research Institute & Department of Structural Biology, SUNY, University at Buffalo, Buffalo, NY, United States, ⁸ Hematology Institute and Blood Bank, Meir Medical Center, Kfar-Saba, Israel, ⁹ Sackler School of Medicine, Tel Aviv University, Tel Aviv, Israel

OPEN ACCESS

Edited by:

Sheue-yann Cheng,
National Cancer Institute (NIH),
United States

Reviewed by:

Mihaly Mezei,
Icahn School of Medicine at Mount
Sinai, United States
Monica Dentice,
University of Naples Federico II, Italy

*Correspondence:

Osnat Ashur-Fabian
osnataf@gmail.com
Dror Tobi
drorto@ariel.ac.il

†Deceased

Specialty section:

This article was submitted to
Cancer Endocrinology,
a section of the journal
Frontiers in Endocrinology

Received: 13 March 2022

Accepted: 26 April 2022

Published: 27 May 2022

Citation:

Tobi D, Krashin E, Davis PJ, Cody V,
Ellis M and Ashur-Fabian O (2022)
Three-Dimensional Modeling of
Thyroid Hormone Metabolites Binding
to the Cancer-Relevant $\alpha\beta 3$ Integrin:
In-Silico Based Study.
Front. Endocrinol. 13:895240.
doi: 10.3389/fendo.2022.895240

Background: Thyroid hormones (TH), T4 and T3, mediate pro-mitogenic effects in cancer cells through binding the membrane receptor $\alpha\beta 3$ integrin. The deaminated analogue tetrac effectively blocks TH binding to this receptor and prevents their action. While computational data on TH binding to the $\alpha\beta 3$ integrin was published, a comprehensive analysis of additional TH metabolites is lacking.

Methods: *In-silico* docking of 26 TH metabolites, including the biologically active thyroid hormones (T3 and T4) and an array of sulfated, deiodinated, deaminated or decarboxylated metabolites, to the $\alpha\beta 3$ receptor binding pocket was performed using DOCK6, based on the three-dimensional representation of the crystallographic structure of the integrin. As the TH binding site upon the integrin is at close proximity to the well-defined RGD binding site, linear and cyclic RGD were included as a reference. Binding energy was calculated for each receptor-ligand complex using Grid score and Amber score with distance movable region protocol.

Results: All TH molecules demonstrated negative free energy, suggesting affinity to the $\alpha\beta 3$ integrin. Notably, based on both Grid and Amber scores sulfated forms of 3,3' T2 (3,3' T2S) and T4 (T4S) demonstrated the highest binding affinity to the integrin, compared to both cyclic RGD and an array of examined TH metabolites. The major thyroid hormones, T3 and T4, showed high affinity to the integrin, which was superior to that of linear RGD. For all hormone metabolites, decarboxylation led to decreased affinity. This corresponds with the observation that the carboxylic group mediates binding to the integrin pocket via divalent cations at the metal-ion-dependent adhesion (MIDAS) motif site. A similar reduced affinity was documented for deaminated forms of T3 (triac) and T4 (tetrac). Lastly, the reverse forms of T3, T3S, and T3AM showed higher Amber scores relative to their native form, indicating that iodination at position 5 is associated with increased binding affinity compared to position 5'.

Summary: Three-dimensional docking of various TH metabolites uncovered a structural basis for a differential computational free energy to the $\alpha\beta$ integrin. These findings may suggest that naturally occurring endogenous TH metabolites may impact integrin-mediate intracellular pathways in physiology and cancer.

Keywords: thyroid hormones, binding energy, integrin, affinity, *in-silico* docking

INTRODUCTION

Thyroid hormones (THs) are essential for the normal development of tissues, as well as for the regulation of cellular metabolism, cell structure and membrane transport (1). Biosynthesis of THs requires several coordinated steps. The prohormone 3,5,3',5' -tetraiodothyronine (T4) is synthesized on thyroglobulin (Tg) in thyroid follicles (2). Iodination of tyrosyl residues and phenolic coupling of the iodotyrosyl residues on Tg by thyroid peroxidase (TPO) forms T4, followed by its proteolytic liberation (3). After delivery to target tissues, T4 undergo deiodination by iodothyronine deiodinases (DIO1, DIO2, and DIO3) to a variety of active and inactive metabolites (4). The removal of one iodine atom from the phenolic (outer) ring of T4 produces the biologically active hormone 3,5,3'-triiodothyronine (T3), whereas removal of an iodine atom from the tyrosyl (inner) ring leads to the formation of a biologically inactive metabolite, 3,3',5'-triiodothyronine also known as reverse T3 (rT3). DIO1 converts T3 into 3,5 diiodothyronine (3,5 T2), while DIO1/DIO3 converts T3 into 3,3' T2. DIO1 and DIO2 also produce 3,3'- T2 by deiodination of the phenolic ring of rT3. Both 3,5 T2 and 3,3' T2 display thyromimetic activity (5, 6). A series of further deiodinations produces 3'-T1 and T0. THs undergo additional metabolic modifications. The conjugation of the phenolic hydroxy group (4'-OH) of T3 and T4 with sulfate and glucuronic acid yields the corresponding sulfated and glucuronidated hormones (7), serving as inactivating pathways of TH action and enhancing their excretion (8, 9). T4 and T3 may further undergo oxidative deamination by transaminase and l-amino acid oxidase to produce their corresponding iodothyroacetic acids, tetrac and triac. Another potential modification, is the removal of the carboxyl group of thyroid hormones (decarboxylation) producing iodothyronamines (TAMs). TAMs may further undergo oxidative deamination by monoamine oxidase to produce the iodothyroacetic acids metabolites. Ether link cleavage by horseradish peroxidase, myeloperoxidase and TPO catalyzes the conversion of T4 into 3,5-diiodotyrosine (DIT) (10–12). The iodine atom from TAMs, iodothyroacetic acids and sulfated THs can be recycled through deiodination (13). TH deiodination and the various metabolic alterations were reviewed and illustrated (14).

TH effects depend on the transcriptional modulation of specific genes, which is mediated *via* nuclear uptake of the biologically active hormone T3, the formation of complexes between T3 and nuclear thyroid hormone receptor (TR) proteins, and the subsequent occupancy of regulatory complexes at thyroid hormone response elements on hormone-

responsive genes (15–17). However, data presented in recent decades support the existence of a number of nongenomic mechanisms of action for the hormone (18, 19). In 2005, a cell surface receptor for thyroid hormone has been identified on the extracellular domain of the $\alpha\beta$ integrin (20). Integrins are a family of 24 structural proteins found in plasma membranes and are essential regulators of cell–cell and cell–extracellular matrix (ECM) protein interactions (21). Integrin $\alpha\beta$ 3 is one of eight integrins with an Arg–Gly–Asp (RGD) recognition site that binds ECM proteins containing this sequence, such as vitronectin, fibronectin and osteopontin (21). The X-ray structure of $\alpha\beta$ 3 has been determined in the presence of Mn^{2+} as a complex with a cyclic RGD peptide (22). Structural data have revealed that the extracellular segment of integrin $\alpha\beta$ 3 is V shaped with the 4-domain α subunit and the 8-domain β subunit bent by 135° (22–24). The RGD peptide occupies a shallow crevice between the propeller and β A domains in the integrin head. A common structural motif observed for integrins is the presence of a metal binding site, termed metal ion-dependent adhesion site (MIDAS) in the integrin α subunit I domain, which binds the divalent cations Mg^{2+}/Mn^{2+} and Ca^{2+} . This site is essential not only for the formation of the integrin heterodimer but also for bridging ligand binding to the integrin. Generally, ligand binding is stimulated by Mg^{2+} or Mn^{2+} and inhibited by Ca^{2+} (25–27).

Subjected to crystallographic modeling (28) and mathematical modelling of the kinetics of thyroid hormone-binding (29) to the extracellular fragment of $\alpha\beta$ 3 integrin, the thyroid hormone receptor on integrin $\alpha\beta$ 3 has been shown to consist of two binding domains. The S1 domain exclusively recognizes T3 and activates PI3K *via* Src kinase. The S2 domain regulates MAPK1 and MAPK2 and binds both T4 and T3. The S2 domain has a higher affinity for T4 than the S1 or S2 sites have for T3. A trophic effect of T4 mediated through the membrane integrin $\alpha\beta$ 3 has been shown experimentally *in vitro* and *in vivo* in cancer cells, leading to induction of proliferation (19, 20, 30–34) and inhibition of apoptosis (32). Tetrac, the deaminated analogue of T4, blocks thyroid hormone-binding at the integrin and inhibits the ability of thyroid hormone analogues to activate MAPK (20). Competition data revealed that RGD peptides also block hormone binding by integrin, suggesting that the hormone-binding site is near the RGD recognition site on $\alpha\beta$ 3 (27, 35).

In recent decades, advances in computational methodologies have enabled virtual docking of small molecules to target sites. Using these methods, ligand conformation that best matches the receptor structure is identified, followed by evaluation of energy of binding (36). The calculated free energy serves as a quantitative predictor of ligand binding affinity (37). In this work, using *in-silico* docking to the $\alpha\beta$ 3 integrin receptor,

binding affinity was assessed for 26 thyroid hormones and their metabolites.

METHODS

A library of 26 thyroid hormones and their metabolites were defined (**Supplementary Figure S1**). These include all active forms of thyroid hormones as well as deiodinated, sulfated, decarboxylated and deaminated metabolites. Three dimensional representations of ligands at physiologic pH were retrieved from the ZINC15 compound database (38), except for reverse T3 sulfate which was retrieved from Pubchem (<https://pubchem.ncbi.nlm.nih.gov/compound/133192#section=3D-Conformer>). Linear RGD and cyclic RGD (cRGD) were used as a reference. *In-silico* docking of molecules to the $\alpha\beta$ integrin RGD binding pocket was performed, based on the three dimensional crystal structure of the integrin (PDB code 1L5G) (23). Briefly, orientations of the ligand relative to a receptor binding cavity were searched using a negative surface image of the target. The image was generated by filling the solvent accessible receptor surface with overlapping spheres and selecting a subset of the spheres to represent the binding site (39). Ligand atoms and spheres were geometrically matched to sample rigid-body orientational space (40), and conformational space of the ligand were sampled in the presence of the receptor binding site *via* the anchor-and-grow incremental construction approach (41) and a grid based score (Grid score) is calculated for each docked molecule (kcal/mol). Next, a more elaborate free energy rescoring step was carried out for each receptor-ligand complex using Amber score. This technique uses the generalized Born/surface area (GB/SA) continuum model for solvation free energy (kcal/mol). Therefore, it provides good estimation of the free energy of the molecules to the receptor with the limitation that configurational entropy effects are ignored. The Amber score is calculated as $E_{Complex} - (E_{Receptor} + E_{Ligand})$, where $E_{Complex}$, $E_{Receptor}$, and E_{Ligand} are molecular mechanics energies combined with the generalized Born and surface area continuum solvation energies (MM-GB/SA) as approximated by the Amber force field (42). The ligand and residues within 4Å from the ligand were defined as fully flexible within the ligand-receptor complex, allowing small structural rearrangements to reproduce the so-called “induced fit” (43) while performing the scoring. Docking and scoring was performed using UCSF DOCK6 software (44). Amber score with distance movable protocol and the following parameters were used: `amber_score_before_md_minimization_cycles 200`, `amber_score_md_steps 6000`, `amber_score_after_md_minimization_cycles 200` doubling the parameters recommended by Brozell et al. to ensure sufficient calculation time (45). Magnesium (Mg^{2+}) atoms were used for MIDAS sites, as its force field parameters are included in DOCK6 package. Protonation state of histidine and other titratable residues was determined using PDB2PQR and if needed amino acids contacting the Mg^{2+} were set to their acidic state manually (46). Docked structure was prepared and results were inspected using UCSF Chimera, a visualization system for exploratory research and analysis (47).

RESULTS

The crystal structure of extracellular segment of the integrin $\alpha\beta$ 3, in complex with cyclic pentapeptide ligand Arg-Gly-Asp-[D-Phe]-[*N*-methyl-Val-] that mimics the natural Arg-Gly-Asp ligand, was used for the docking calculations. Evaluation of the docking procedure was carried out by docking the cyclic pentapeptide ligand to its binding site in the integrin. **Figure 1** presents the crystallographic structure of the Arg-Gly-Asp ligand (carbon atoms colored gold) in the integrin $\alpha\beta$ 3 binding site vs. the docked structure (carbon atoms colored cyan). The Arg and Asp ligand side chains are marked with orange arrowhead. The carboxyl groups of crystallographic and docked structure are almost overlapping and interact with the Mg^{2+} atoms (green sphere). Both arginine side chains of the crystallographic and docked structure contact Asp218 and their nitrogen atoms are 3.6Å apart. The calculated docking Grid score is -81.85 and the rescoring step with Amber force field resulted in Amber score of -58.30. The negative scores indicate good affinity of the RGD ligand to the integrin binding site. In comparison the cyclic RGD, the linear RGD molecule displays a significantly lower amber score (-33.82). The overall good overlap between the crystallographic and docked structure and the accepted scores indicate the ability of the DOCK6 package and the parameters we used to correctly dock and score ligand to the integrin binding site.

We next performed docking to a library of 26 thyroid hormones and their metabolites and two RGD ligands (cyclic and linear peptides). The free energies for the molecules in our model are summarized in **Table 1**. The best four scoring molecules (lowest Amber score) are depicted in **Figure 2A**, and the worst four scoring molecules (highest Amber score) are depicted in **Figure 2B**. The prohormone T4 and the biologically active hormone T3, are among top scoring compounds, substantiating previously published work which positioned both molecules as key $\alpha\beta$ 3 integrin ligands (17). Notably, all the best four ranking molecules have a carboxyl group attached to the inner ring *via* two-carbon linker, while all the worst four ranking molecules are missing this group. The docked structure of sulfated T4 (T4S) with an amber score of -69.37 and decarboxylated T4 (T4AM) with an amber score of -21.19, are presented in **Figures 3A, B**, respectively. T4S interacts with one Mg^{2+} atom of the MIDAS sites through the carboxylic group and with another Mg^{2+} atom through the sulfate group, while T4AM does not closely interact with any of the Mg^{2+} atoms. This results in a reverse binding orientation of the two molecules. The docked structures of the best four scoring molecules are depicted in **Figure 3C** using wire representation, while the negatively charged oxygens of the carboxylic and sulfate groups are presented as red spheres. These negatively charged oxygens form electrostatic interactions with the Mg^{2+} atoms at the MIDAS site (green spheres). Thus, our model demonstrates the central role of metal ions as essential to thyroid hormones binding. Support that the negatively charged sulfates increase binding affinity to the integrin is provided by the higher amber score for sulfated T4 (T4S) and 3,3'T2 (3,3'T2S) in

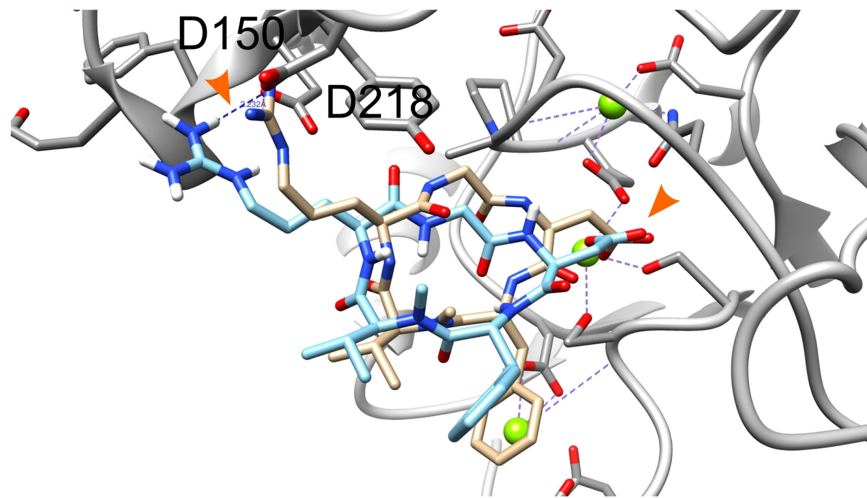


FIGURE 1 | Docking of the cyclic pentapeptide ligand Arg-Gly-Asp-[D-Phe]-[N-methyl-Val-] to integrin α v β 3. Integrin's binding site backbone (ribbons) and side chains (sticks) are colored gray with oxygen atoms in red and nitrogen in blue. The crystallography and docked structures of the cyclic peptide Arg-Gly-Asp-[D-Phe]-[N-methyl-Val-] are shown using stick representations with carbon atoms colored gold and cyan, respectively. Oxygen, nitrogen, and hydrogen atoms are colored red, blue and white, respectively. Mg^{2+} atoms are shown as green spheres. Ligand side chains Arg and Asp are marked with orange arrowhead.

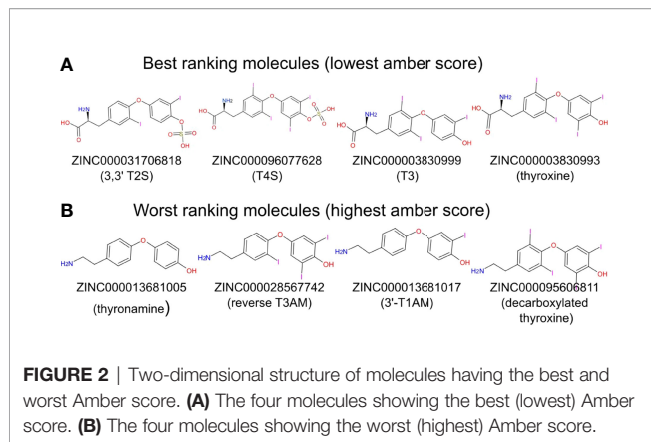
TABLE 1 | Grid Amber score for thyroid hormone metabolites.

| Molecule | Grid_Score kcal/mol | Amber_Score kcal/mol |
|--|---------------------|----------------------|
| ZINC000031706818 (3,3' T2S, sulfated) ¹ | -68.63 | -76.90 |
| ZINC000096077628 (T4S, sulfated) | -76.41 | -69.37 |
| RGDc ² | -81.85 | -58.30 |
| ZINC000003830999 (3,3', 5 T3, triiodothyronine) | -53.40 | -51.72 |
| ZINC000003830993 (T4, thyroxine) | -51.76 | -42.96 |
| ZINC000004097417 (reverse T3) | -53.19 | -42.84 |
| ZINC000085552312 (T3S, sulfated) | -65.81 | -42.20 |
| ZINC000013681007 (3T1AM, decarboxylated) | -40.60 | -41.22 |
| ZINC000085627494 (3',5' T2) | -59.25 | -40.80 |
| ZINC000016051523 (3,3' T2) | -52.95 | -40.33 |
| ZINC000013681015 (3',5' T2AM, decarboxylated) | -42.16 | -37.02 |
| ZINC000006092925 (3'-T1) | -51.31 | -35.13 |
| ZINC000002387178 (3-T1) | -45.79 | -35.01 |
| ZINC000003922521 (RGD) ³ | -89.10 | -33.82 |
| ZINC000008681598 (tetrac, deaminated) | -63.63 | -29.13 |
| ZINC000004258247 (3,5 T2) | -46.02 | -28.90 |
| ZINC000000001575 (MIT - 3 iodotyrosine) | -45.15 | -28.58 |
| ZINC000003861723 (DIT - 3,5 Diiodotyrosine) | -54.26 | -25.85 |
| ZINC000028569157 (T3AM, decarboxylated) | -43.49 | -25.64 |
| reverse T3S (reverse T3, sulfated) | -67.65 | -24.77 |
| ZINC000000403598 (T0 - thyronine) | -46.88 | -24.42 |
| ZINC000004217580 (triac, deaminated) | -61.18 | -24.15 |
| ZINC000013681013 (3,3'-T2AM, decarboxylated) | -45.96 | -23.61 |
| ZINC000013681010 (3,5 T2AM, decarboxylated) | -41.32 | -23.17 |
| ZINC000013681005 (T0AM, decarboxylated) | -39.78 | -22.47 |
| ZINC000028567742 (reverse T3AM, decarboxylated) | -44.74 | -22.23 |
| ZINC000013681017 (3'-T1AM, decarboxylated) | -43.50 | -22.21 |
| ZINC000095606811 (T4AM - decarboxylated) | -44.02 | -21.19 |

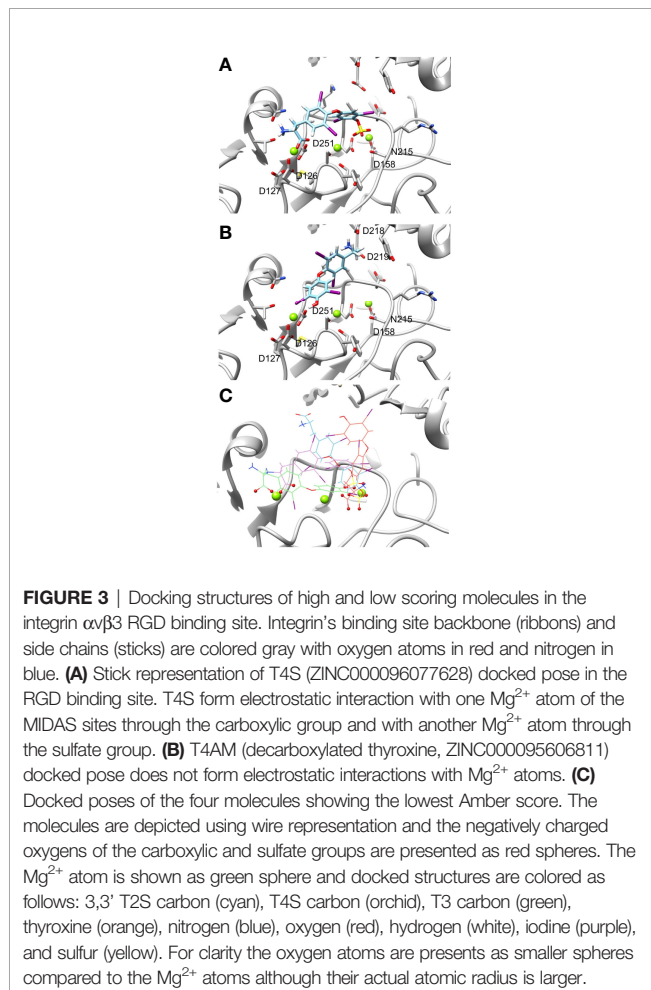
¹ZINC database ID and common name in parentheses are given for each molecule whenever possible.

²cyclic pentapeptide Arg-Gly-Asp-[D-Phe]-[N-methyl-Val-]s.

³linear Arg-Gly-Asp peptide.



comparison to the non-sulfated hormones (**Table 1**). However, an exception was observed for T3S, in which amber score was higher compared to the non-sulfated metabolite, with the carboxylic group flipped away from the MIDAS site. Docking for T4 and T3 compared to their sulfated forms is depicted in **Figure 4**.



We further observed that thyroid hormones have increased affinity compared to their reverse form. Reverse T3 (rT3) is the metabolically inactive form of T3. In our calculation we show that the Amber score of T3 is -51.72 while that of reverse T3 is -42.84. Thus, reverse T3 has a smaller affinity to integrin $\alpha\beta$ 3 binding site compared with that of T3. The docking poses of T3 (cyan) and reverse T3 (pink) are presented in **Figure 5A**, demonstrating different binding conformations. Despite the different poses, there is a steric clash between the T3 and reverse T3 docked structures. Thus, a competitive binding of the two hormones to the integrin $\alpha\beta$ 3 binding site is postulated. Similarly, the Amber score of T3S is -42.20 and that of reverse T3S is -24.77 and the Amber score of T3AM is -25.64 and that of reverse T3AM -22.23. That is, in general iodination in positions 3,5, and 3' increase the affinity of the hormone compared to iodination at positions 3, 3', and 5'. **Figure 5B** shows the docked structures of T3 (cyan), T3S (pink), and T3AM (green). These three molecules have different binding poses to the integrin $\alpha\beta$ 3 site, making the hypothesis that iodination in positions 3,5, and 3' results in a better fit of these molecules to the binding site less likely. Another possible explanation is that iodination in positions 3,5, and 3' results in improved intrinsic binding ability. Space filling model of T3 and reverse T3 are presented in **Figure 5C**. The two iodine atoms in positions 3 and 5 of T3 on the inner ring tether the outer ring and restrict its rotation ability, along the single bonds connecting the two rings, as their size is comparable to the size of the ring itself. While the two iodine atoms in position 3' and 5' of the outer ring do not restrict its rotation ability along the single bonds connecting the two rings. Thus, iodine atoms at positions 3 and 5 rigidify the hormones. If this rigidification locks the molecules in their bound conformation it can increase their affinity to the receptor.

Lastly, the deaminated forms of T3 (triac) and T4 (tetrac) display higher amber scores compared to the native hormones (**Table 1**). In details, while T3 and T4 have amber scores of -51.72 and -42.96, respectively, the calculated score of triac and tetrac was -24.15 and -29.13, respectively. This suggests a role for the amine group in the interaction with the integrin receptor. **Figures 6A, B** show in close up the amine and carboxyl groups of T4 and T3, respectively. The carboxylic group of T4 contact Mg^{2+} atom while the amine group form hydrogen bond with the backbone carbonyl of N215. Similarly, the carboxyl group of T3 contact another Mg^{2+} atom while the amine group form electrostatic interaction with N313. Thus, the two groups contribute to the binding affinity of T4 and T3.

DISCUSSION

For many years thyroid hormones were considered to act *via* genomic actions, initiated by direct binding of the biologically active hormone T3 to its nuclear thyroid receptors (15). For these activities, T4 has significant lower affinities and is considered merely a prohormone. This dogma was challenged once a discrete binding site for both T3 and T4 was discovered upon a membrane receptor with multiple roles in physiology and

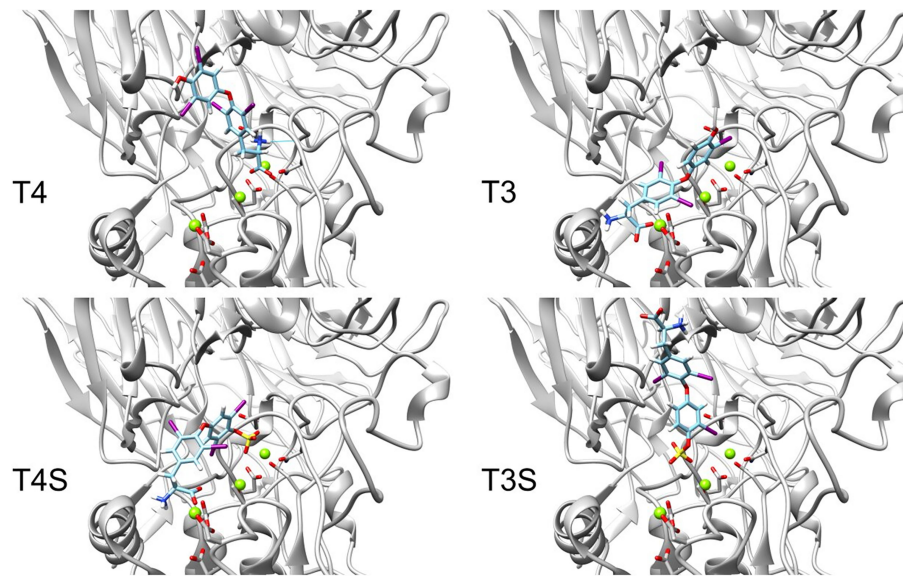


FIGURE 4 | Docking structures of T4, T3 to the integrin $\alpha\beta$ 3 binding site in comparison to their sulfated forms. Integrin's binding site backbone (ribbons) and side chains (sticks) are colored gray with oxygen atoms in red and nitrogen in blue. Comparison between the docked structure of T3 (ZINC000003830999), T4 (ZINC000003830993), sulfated T3 (ZINC000031706818) and sulfated T4 (ZINC000096077628) in the $\alpha\beta$ 3 binding site. The molecules are depicted using stick representation. The Mg^{2+} atom is shown as green sphere and docked structures are colored as follows: carbon (cyan), nitrogen (blue), oxygen (red), hydrogen (white), iodine (purple), and sulfur (yellow).

malignancies, namely the $\alpha\beta$ 3 integrin (17). This discovery was the first to demonstrate that small molecules can serve as ligands for this integrin. Since then, ample preclinical data in cell lines

and animal models confirmed an array of functional consequences for this novel non-genomic signaling pathway (48). This highlights the importance of developing drugs targeting the hormone binding site upon the integrin.

Direct attachment of both T3 and T4 was validated not only by binding experiments with purified $\alpha\beta$ 3 protein (20, 30, 49), but also by computational modeling. In this current study the binding conformations of the various hormone metabolites relative to the RGD binding pocket, revealed that T3 and its decarboxylated (T3AM) and sulfated (T3S) forms bind at close proximity to the RGD pocket. The results for T3 are supported by experimental work indicating that RGD hinders T3 binding to its exclusive S1 site upon the $\alpha\beta$ 3 integrin (49). In contrast, T4 and rT3, which similarly affects cancer proliferation *via* the integrin (50), are located at a different binding pocket which is farther from the RGD site. Notably, decarboxylated T4 (T4AM) binding also overlaps with a site close to the RGD pocket, while its sulfated form (T4S) intersects with both the RGD and T4 sites. Combined with their low calculated free energy and expected lack of activity (8, 9), this suggests that the sulfated forms of T4 and T3 may act as novel potential blockers for the RGD and hormone integrin sites. Cody et al. mapped binding of T4 and its deaminated form, tetrac, to the RGD site in the integrin pocket (35). This preliminary modeling study also indicated that due to the smaller overall length of the thyroid hormone compared with the RGD peptide, the hormone can occupy the RGD binding site, mostly by interacting with the β A domain in the extracellular domain of the integrin, and not *via* the Arg recognition site in the α v propeller domain. A later study further combined quantum mechanical-molecular mechanical (QM/MM) molecular dynamics simulations and characterized the intermolecular

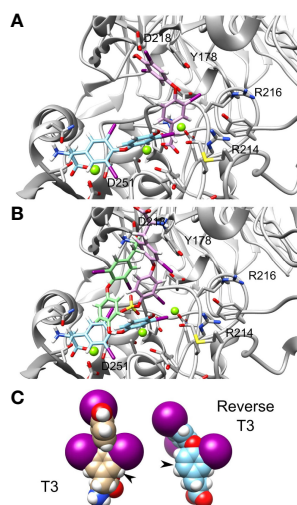


FIGURE 5 | T3 and reverse T3 docked structures. Integrin's binding site backbone (ribbons) and side chains (sticks) are colored gray with oxygen atoms in red and nitrogen in blue. **(A)** The docked structure of T3 (ZINC000003830999) and reverse T3 (ZINC000004097417) in the $\alpha\beta$ 3 binding site. Atom coloring scheme is as follows: T3 carbon (cyan), reverse T3 carbon (pink), iodine (purple), oxygen (red), nitrogen (blue), and hydrogen (white). **(B)** Docked structures of T3, T3S (pink), and T3AM (green). Carbon colors are: T3 (cyan), T3S (pink), and T3AM (green). **(C)** Space filling model of T3 and reverse T3.

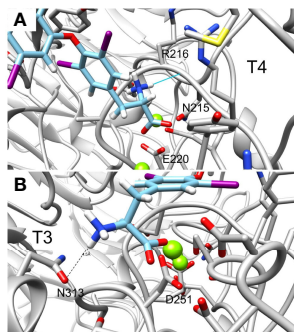


FIGURE 6 | Close up of the amine and carboxylic groups of T3 and T4 docked structures. Integrin's binding site backbone (ribbons) and side chains (sticks) are colored gray with oxygen atoms in red and nitrogen in blue. **(A)** T4 amine group forms hydrogen bond with N215 backbone carbonyl while the carboxyl group form electrostatic interaction with Mg^{2+} atom. **(B)** Similarly, T3 amine group form electrostatic interaction with N313 and the carboxyl group with Mg^{2+} . Docked structures are colored as follows: carbon (cyan), nitrogen (blue) oxygen (red), hydrogen (white), and iodine (purple).

interactions for T3, T4, tetrac and a series of hormone analogues (27). These data revealed that T3, T4 and tetrac may occupy two alternate sites in the integrin RGD binding pocket. In one orientation of the T4, the 4'-hydroxyphenyl ring occupies a binding pocket deeper within the crevice between the $\alpha\beta$ 3 domains, while in the other binding mode, the phenolic ring occupies the interface between the integrin $\alpha\beta$ 3 domains. For T3 the tyrosyl moiety may lay along the Arg side chain of the cyclic RGD peptide, or places the 4'-phenolic ring in a different binding pocket than observed for T4. The results for tetrac reveal one orientation which aligns similar to T3 along the side chain of Arg in the RGD peptide binding site, while in the other binding mode tetrac's phenolic ring binds deeper within the RGD binding pocket, similar to that of T4.

The biological thyroid hormones, T3 and T4, were among the molecules with the lowest calculated interaction energy with $\alpha\beta$ 3. This, together with the observation that the majority of T3 and T4 catabolized metabolites display significantly reduced binding affinity to the integrin, substantiates that the major integrin ligands are the native thyroid hormones. Based on the calculated free energy, T3 has higher affinity to the integrin compared to T4. These results are in accord with Freindorf et al., who suggested that an additional iodine atom in T4 may affect its interaction with the protein (27). However, as the prohormone T4 is produced at significantly higher physiological concentrations compared to T3 (13), it is positioned as the major endogenous ligand for the $\alpha\beta$ 3 integrin. This was confirmed by binding assays using physiological and supra physiological concentrations of both hormones (20, 30, 49).

The best ranking molecules in our model are carboxylated, while the worst ranking molecules lack this group. This result may be explained by the interaction of the carboxylic group with the Mg^{2+} atom in the integrin MIDAS site, which is absent in the decarboxylated compounds. Moreover, the top binding

compounds were sulfated forms of 3,3' T2 (T2S) and T4 (T4S). *In silico* docking for these best scoring compounds demonstrated that the negatively charged oxygen of the sulfate group interacts with another Mg^{2+} atom of the MIDAS sites. This may also explain the reverse orientation between sulfated T4 (T4S) and decarboxylated T4 (T4AM), as well as that of sulfated T3 in comparison to the non-sulfated form. The addition of sulfate at position 4' enable the molecule to bind *via* its negatively charge sulfate and carboxylic groups with the Mg^{2+} atoms. Removal of these two negative groups at T4AM results in a change of orientation that moves the positively charged amine group away from the Mg^{2+} atoms and bring it close to Asp218 and Asp219 to contacts these negatively charges amino acids. Collectively, our results provide support that the metal ions in the $\alpha\beta$ 3 integrin domain are essential to thyroid hormone binding. This is in accordance with the well-defined characteristic of integrins, in which ligand binding is dependent upon bivalent cations (25, 26). However, the effect of sulfate on interaction with the integrin MIDAS domain should be further elucidated, as sulfated T3 did not display increased affinity compared to the non-sulfated hormone. We further observed that iodine localization in the hormones affects binding affinity to the integrin. Reverse forms of T3, sulfated T3 and decarboxylated T3 demonstrated significantly higher free energy compared to their native forms. Based on space filling model for T3 and reverse T3 we identified that the iodine atoms in positions 3 and 5 on the inner ring restrict rotation ability and rigidify and locks the hormone bound conformation. This results in increased affinity to the integrin receptor. In contrast, the two iodine atoms in position 3' and 5' of the outer ring, observed in the reverse forms, do not display such capabilities. Lastly, the deaminated forms of T3 (triac) and T4 (tetrac) present lower affinity to the integrin compared with the native hormones. This observation, which was reported before by Freindorf et al. (27), stresses the importance of the NH2 group in the interaction between the ligands and the integrin.

To conclude, by performing a comprehensive three-dimensional docking for thyroid hormone and an array of naturally occurring endogenous metabolites, we have identified that their binding to the $\alpha\beta$ 3 integrin is affected by several structure-related characteristics. As the involvement of the thyroid hormone-integrin axis in cancer progression and inhibition is gaining more attention, this study may lead to better understanding of the tumor promoting effects of various thyroid dysfunction conditions, as well as to the development of effective inhibitors to the integrin site.

AUTHOR'S NOTE

This article is dedicated to the memory of Dr Eilon Krashin, a brilliant physician, researcher and a friend.

DATA AVAILABILITY STATEMENT

The original contributions presented in the study are included in the article/**Supplementary Material**. Further inquiries can be directed to the corresponding authors.

AUTHOR CONTRIBUTIONS

DT, EK, and OA-F designed this study. DT performed the docking. DT, ME, PD, VC, and OA-F wrote, read and approved the manuscript.

REFERENCES

- Moeller L, Fuhrer D. Thyroid Hormone, Thyroid Hormone Receptors, and Cancer: A Clinical Perspective. *Endocrine-Related Cancer* (2013) 20:R19–29. doi: 10.1530/ERC-12-0219
- Saber-Lichtenberg Y, Brix K, Schmitz A, Heuser JE, Wilson JH, Lorand L, et al. Covalent Cross-Linking of Secreted Bovine Thyroglobulin by Transglutaminase. *FASEB J* (2000) 14:1005–14. doi: 10.1096/fasebj.14.7.1005
- Ekhholm R. Biosynthesis of Thyroid Hormones. *Int Rev Cytol* (1990) 120:243–88. doi: 10.1016/S0074-7696(08)61602-2
- Wu SY, Green WL, Huang WS, Hays MT, Chopra IJ. Alternate Pathways of Thyroid Hormone Metabolism. *Thyroid* (2005) 15:943–58. doi: 10.1089/thy.2005.15.943
- Lanni A, Moreno M, Cioffi M, Goglia F. Effect of 3, 3'-Di-Iodothyronine and 3, 5-Di-Iodothyronine on Rat Liver Mitochondria. *J Endocrinol* (1993) 136:59–64. doi: 10.1677/joe.0.1360059
- Senese R, De Lange P, Petito G, Moreno M, Goglia F, Lanni A. 3, 5-Diiodothyronine: A Novel Thyroid Hormone Metabolite and Potent Modulator of Energy Metabolism. *Front Endocrinol* (2018) 9:427. doi: 10.3389/fendo.2018.00427
- Visser TJ. Role of Sulfation in Thyroid Hormone Metabolism. *Chemico-biological Interact* (1994) 92:293–303. doi: 10.1016/0009-2797(94)90071-X
- Rikke BA, Roy AK. Structural Relationships Among Members of the Mammalian Sulfotransferase Gene Family. *Biochim Biophys Acta* (1996) 1307:331–8. doi: 10.1016/0167-4781(96)00065-6
- Falany CN. Sulfation and Sulfotransferases. Introduction: Changing View of Sulfation and the Cytosolic Sulfotransferases. *FASEB J* (1997) 11:1–2. doi: 10.1096/fasebj.11.1.9034159
- Jolin T, Morreale De Escobar G. Deiodination of L-thyroxine and its Activity on the Oxidation *In Vitro* of Reduced Nicotinamide-Adenine Dinucleotide by Peroxidase Plus Hydrogen Peroxide. *Biochem J* (1971) 125:869–78. doi: 10.1042/bj1250869
- Burger AG, Engler D, Buergi U, Weissel M, Steiger G, Ingbar SH, et al. Ether Link Cleavage is the Major Pathway of Iodothyronine Metabolism in the Phagocytosing Human Leukocyte and Also Occurs *In Vivo* in the Rat. *J Clin Invest* (1983) 71:935–49. doi: 10.1172/JCI110848
- Kubota K, Uchimura H, Mitsuhashi T, Chiu SC, Kuzuya N, Ito K, et al. Peroxidatic Degradation and Ether Link Cleavage of Thyroxine in a Particulate Fraction of Human Thyroid. *Life Sci* (1985) 36:1033–9. doi: 10.1016/0024-3205(85)90488-6
- Mondal S, Raja K, Schweizer U. Chemistry and Biology in the Biosynthesis and Action of Thyroid Hormones. *Angew Chem Int Ed Engl* (2016) 55:7606–30. doi: 10.1002/anie.201601116
- Köhrle J. The Colorful Diversity of Thyroid Hormone Metabolites. *Eur Thyroid J* (2019) 8:115–29. doi: 10.1159/000497141
- Brent GA. Mechanisms of Thyroid Hormone Action. *J Clin Invest* (2012) 122:3035–43. doi: 10.1172/JCI60047
- Abdalla SM, Bianco AC. Defending Plasma T3 is a Biological Priority. *Clin Endocrinol* (2014) 81:633–41. doi: 10.1111/cen.12538
- Davis PJ, Goglia F, Leonard JL. Nongenomic Actions of Thyroid Hormone. *Nat Rev Endocrinol* (2016) 12:111–21. doi: 10.1038/nrendo.2015.205
- Cheng SY, Leonard JL, Davis PJ. Molecular Aspects of Thyroid Hormone Actions. *Endocr Rev* (2010) 31:139–70. doi: 10.1210/er.2009-0007
- Davis PJ, Davis FB, Mousa SA, Luidens MK, Lin HY. Membrane Receptor for Thyroid Hormone: Physiologic and Pharmacologic Implications. *Annu Rev Pharmacol Toxicol* (2011) 51:99–115. doi: 10.1146/annurev-pharmtox-010510-100512
- Bergh JJ, Lin HY, Lansing L, Mohamed SN, Davis FB, Mousa S, et al. Integrin α V β 3 Contains a Cell Surface Receptor Site for Thyroid Hormone That is Linked to Activation of Mitogen-Activated Protein Kinase and Induction of Angiogenesis. *Endocrinology* (2005) 146:2864–71. doi: 10.1210/en.2005-0102
- Plow EF, Haas TA, Zhang L, Loftus J, Smith JW. Ligand Binding to Integrins. *J Biol Chem* (2000) 275:21785–8. doi: 10.1074/jbc.R000003200
- Xiong JP, Stehle T, Diefenbach B, Zhang R, Dunker R, Scott DL, et al. Crystal Structure of the Extracellular Segment of Integrin α V β 3. *Science* (2001) 294:339–45. doi: 10.1126/science.1064535
- Xiong JP, Stehle T, Zhang R, Joachimiak A, Frech M, Goodman SL, et al. Crystal Structure of the Extracellular Segment of Integrin α V β 3 in Complex With an Arg-Gly-Asp Ligand. *Science* (2002) 296:151–5. doi: 10.1126/science.1069040
- Arnaout MA, Mahalingam B, Xiong JP. Integrin Structure, Allostery, and Bidirectional Signaling. *Annu Rev Cell Dev Biol* (2005) 21:381–410. doi: 10.1146/annurev.cellbio.21.090704.151217
- Pelletier AJ, Kunicki T, Quaranta V. Activation of the Integrin α V β 3 Involves a Discrete Cation-Binding Site That Regulates Conformation (*). *J Biol Chem* (1996) 271:1364–70. doi: 10.1074/jbc.271.3.1364
- Cierniewska-Cieslak A, Cierniewski CS, Bledzka K, Papierak M, Michalec L, Zhang L, et al. Identification and Characterization of Two Cation Binding Sites in the Integrin β 3 Subunit. *J Biol Chem* (2002) 277:11126–34. doi: 10.1074/jbc.M112388200
- Freindorf M, Furlani TR, Kong J, Cody V, Davis FB, Davis PJ. Combined QM/MM Study of Thyroid and Steroid Hormone Analogue Interactions With α V β 3 Integrin. *J BioMed Biotechnol* (2012) 2012:959057. doi: 10.1155/2012/959057
- Lin HY, Cody V, Davis FB, Hercbergs AA, Luidens MK, Mousa SA, et al. Identification and Functions of the Plasma Membrane Receptor for Thyroid Hormone Analogues. *Discovery Med* (2011) 11:337–47.
- Lin HY, Landersdorfer CB, London D, Meng R, Lim CU, Lin C, et al. Pharmacodynamic Modeling of Anti-Cancer Activity of Tetraiodoacetic Acid in a Perfused Cell Culture System. *PLoS Comput Biol* (2011) 7:e1001073. doi: 10.1371/journal.pcbi.1001073
- Davis FB, Tang HY, Shih A, Keating T, Lansing L, Hercbergs A, et al. Acting Via a Cell Surface Receptor, Thyroid Hormone Is a Growth Factor for Glioma Cells. *Cancer Res* (2006) 66:7270–5. doi: 10.1158/0008-5472.CAN-05-4365
- Lin HY, Tang HY, Shih A, Keating T, Cao G, Davis PJ, et al. Thyroid Hormone Is a MAPK-dependent Growth Factor for Thyroid Cancer Cells and is Anti-Apoptotic. *Steroids* (2007) 72:180–7. doi: 10.1016/j.steroids.2006.11.014
- Lin HY, Tang HY, Keating T, Wu YH, Shih A, Hammond D, et al. Resveratrol Is Pro-Apoptotic and Thyroid Hormone is Anti-Apoptotic in Glioma Cells: Both Actions Are Integrin and ERK Mediated. *Carcinogenesis* (2008) 29:62–9. doi: 10.1093/carcin/bgm239
- Luidens MK, Mousa SA, Davis FB, Lin HY, Davis PJ. Thyroid Hormone and Angiogenesis. *Vascul Pharmacol* (2010) 52:142–5. doi: 10.1016/j.vph.2009.10.007
- Davis PJ, Glinsky GV, Lin HY, Leith JT, Hercbergs A, Tang HY, et al. Cancer Cell Gene Expression Modulated From Plasma Membrane Integrin α V β 3 by Thyroid Hormone and Nanoparticulate Tetrac. *Front Endocrinol (Lausanne)* (2014) 5:240. doi: 10.3389/fendo.2014.00240
- Cody V, Davis PJ, Davis FB. Molecular Modeling of the Thyroid Hormone Interactions With α V β 3 Integrin. *Steroids* (2007) 72:165–70. doi: 10.1016/j.steroids.2006.11.008
- Kitchen DB, Decornez H, Furr JR, Bajorath J. Docking and Scoring in Virtual Screening for Drug Discovery: Methods and Applications. *Nat Rev Drug Discovery* (2004) 3:935–49. doi: 10.1038/nrd1549
- Wan S, Bhati AP. Rapid, Accurate, Precise and Reproducible Ligand-Protein Binding Free Energy Prediction. *Interface Focus* (2020) 10:20200007. doi: 10.1098/rsfs.2020.0007
- Sterling T, Irwin JJ. Zinc 15–Ligand Discovery for Everyone. *J Chem Inf Model* (2015) 55:2324–37. doi: 10.1021/acs.jcim.5b00559

SUPPLEMENTARY MATERIAL

The Supplementary Material for this article can be found online at: <https://www.frontiersin.org/articles/10.3389/fendo.2022.895240/full#supplementary-material>

39. Kuntz ID, Blaney JM, Oatley SJ, Langridge R, Ferrin TE. A Geometric Approach to Macromolecule-Ligand Interactions. *J Mol Biol* (1982) 161:269–88. doi: 10.1016/0022-2836(82)90153-X
40. Ewing TJ, Kuntz ID. Critical Evaluation of Search Algorithms for Automated Molecular Docking and Database Screening. *J Comput Chem* (1997) 18:1175–89. doi: 10.1002/(SICI)1096-987X(19970715)18:9<1175::AID-JCC6>3.0.CO;2-O
41. Ewing TJ, Makino S, Skillman AG, Kuntz ID. Dock 4.0: Search Strategies for Automated Molecular Docking of Flexible Molecule Databases. *J Comput Aided Mol Des* (2001) 15:411–28. doi: 10.1023/A:1011115820450
42. Graves AP, Shivakumar DM, Boyce SE, Jacobson MP, Case DA, Shoichet BK. Rescoring Docking Hit Lists for Model Cavity Sites: Predictions and Experimental Testing. *J Mol Biol* (2008) 377:914–34. doi: 10.1016/j.jmb.2008.01.049
43. Xu M, Lill MA. Induced Fit Docking, and the Use of QM/MM Methods in Docking. *Drug Discovery Today Technol* (2013) 10:e411–418. doi: 10.1016/j.ddtec.2013.02.003
44. Lang PT, Brozell SR, Mukherjee S, Pettersen EF, Meng EC, Thomas V, et al. DOCK 6: Combining Techniques to Model RNA-small Molecule Complexes. *Rna* (2009) 15:1219–30. doi: 10.1261/rna.1563609
45. Brozell SR, Mukherjee S, Balias TE, Roe DR, Case DA, Rizzo RC. Evaluation of DOCK 6 as a Pose Generation and Database Enrichment Tool. *J Comput Aided Mol Des* (2012) 26:749–73. doi: 10.1007/s10822-012-9565-y
46. Dolinsky TJ, Nielsen JE, Mccammon JA, Baker NA. PDB2PQR: An Automated Pipeline for the Setup of Poisson-Boltzmann Electrostatics Calculations. *Nucleic Acids Res* (2004) 32:W665–667. doi: 10.1093/nar/gkh381
47. Pettersen EF, Goddard TD, Huang CC, Couch GS, Greenblatt DM, Meng EC, et al. Ucsf Chimera—A Visualization System for Exploratory Research and Analysis. *J Comput Chem* (2004) 25:1605–12. doi: 10.1002/jcc.20084
48. Davis PJ, Mousa SA, Lin H-Y. Nongenomic Actions of Thyroid Hormone: The Integrin Component. *Physiol Rev* (2021) 101:319–52. doi: 10.1152/physrev.00038.2019
49. Lin H-Y, Sun M, Tang H-Y, Lin C, Luidens MK, Mousa SA, et al. L-Thyroxine vs. 3, 5, 3'-triiodo-L-thyronine and Cell Proliferation: Activation of Mitogen-Activated Protein Kinase and Phosphatidylinositol 3-Kinase. *Am J Physiology-Cell Physiol* (2009) 296(5):C980–91. doi: 10.1152/ajpcell.00305.2008
50. Lin HY, Tang HY, Leinung M, Mousa SA, Hercbergs A, Davis PJ. Action of Reverse T3 on Cancer Cells. *Endocr Res* (2019) 44:148–52. doi: 10.1080/07435800.2019.1600536

Conflict of Interest: The authors declare that the research was conducted in the absence of any commercial or financial relationships that could be construed as a potential conflict of interest.

Publisher's Note: All claims expressed in this article are solely those of the authors and do not necessarily represent those of their affiliated organizations, or those of the publisher, the editors and the reviewers. Any product that may be evaluated in this article, or claim that may be made by its manufacturer, is not guaranteed or endorsed by the publisher.

Copyright © 2022 Tobi, Krashin, Davis, Cody, Ellis and Ashur-Fabian. This is an open-access article distributed under the terms of the Creative Commons Attribution License (CC BY). The use, distribution or reproduction in other forums is permitted, provided the original author(s) and the copyright owner(s) are credited and that the original publication in this journal is cited, in accordance with accepted academic practice. No use, distribution or reproduction is permitted which does not comply with these terms.